

Subspace Modeling of Multi-User MIMO Channels

Nicolai Czik¹, Bernd Bandemer², Claude Oestges³, Thomas Zemen¹, Arogyaswami Paulraj²

¹FTW Forschungszentrum Telekommunikation Wien, Vienna, Austria

²Smart Antennas Research Group, Stanford University, USA

³ICTEAM, Université catholique de Louvain, Louvain-la-Neuve, Belgium

Abstract—In multiple-input multiple-output (MIMO) systems, the propagation channels can be characterized by their spatial structure, described by the (complex-valued) channel correlation. Accordingly, also interference in MIMO systems is likely to occur in a spatially structured, correlated way.

We discuss that structured spatial interference affects mutual information under interference, depending on the eigenspace alignment between the channel of the desired signal and the channel carrying the interference. Intuitively, worst-case interference occurs, when the channels from the intended signal and the interference show a similar spatial structure. In contrast, least hurtful interference is encountered when these channels are maximally non-aligned.

In this paper, we develop an analytical channel model generating multi-user MIMO channels with a given degree of severity of interference, described by the alignment of the channels' eigenspaces. Using radio channel measurements, we parameterize our model to reflect realistic scenarios.

I. INTRODUCTION

With multiple-input multiple-output (MIMO) systems penetrating the mass market, the number of multi-antenna devices increases drastically. As a result, the interference from MIMO devices is constantly growing.

Current deployments of MIMO focus on single-user schemes, where MIMO devices are orthogonally addressed, either by time-division or frequency-division multiplex. Future deployments are expected to support space-division multiplex, thus transmitting to or receiving from multiple MIMO users at the same time. This is feasible when the channels to the different users are sufficiently orthogonal in the signal domain.

The influence of interference on MIMO systems was previously studied. For example, Blum published a survey article on MIMO transmission under interference, which includes mutual information expressions [1].

The authors would like to thank Prof. George Papanicolaou, Stanford University, for enlightening discussions on curves in the unitary group.

This work was partially supported by the European Commission in the framework of the FP7 Network of Excellence in Wireless COMMunications NEWCOM++ (contract no. 216715) and of the FP7 STREPS BuNGee (contract no. 248267), by the Vienna Science and Technology Fund in the FTW project PUCCO, by the Austrian Science Fund (FWF) through grant S10607, and by the European COST 2100 Action. The FTW Forschungszentrum Telekommunikation Wien is supported by the Austrian Government and the City of Vienna within the competence center program COMET. The work of C. Oestges is supported by the Belgian Fonds de la Recherche Scientifique (FRS-FNRS). The work of N. Czik was partially supported by an Erwin Schrodinger Fellowship of the Austrian Science Fund (FWF grant number J2789-N14). The work of B. Bandemer is supported by an Eric and Illeana Benhamou Stanford Graduate Fellowship.

Several publications have discussed *signal-processing algorithms* that consider colored noise. Liu et al. [2] have presented an optimum training signal design for correlated MIMO channels under colored interference. However, the simplifying assumption is made that all transmitted signals, regardless of their origin, result in the same receive correlation. The suppression of (strongly correlated) directional interference is discussed in [3]. The authors model the interference as a rank-one signal from a single direction, but this assumption is not supported by real-world measurements. Recently, Rahman et al. [4] discussed the impact of different kinds of interfering signals. It was shown that interference from a space-time coded signal is worst (but can be mitigated with appropriate algorithms). However, the authors used the rich-scattering assumption for both the desired and the interfering signal, which is equivalent to spatially white interference.

Very few previous studies have attempted to *model* correlated interference. A ray-tracing approach is presented in [5], where the authors accurately model an urban scenario with multiple base stations and mobile stations. This modeling approach appears very promising, but the results have not been validated against measurements.

Poutanen et al. [6] introduced a promising geometry-based stochastic approach of “common scatterers”, which was adopted by the European COST 2100 model. This idea extends previous cluster-based channel models to include some clusters that are visible only to specific users, while others are visible to all users, which induces correlation between the channels at different users. The authors also exemplify a possible parametrization from a limited set of measurements.

However, to the best of the authors' knowledge, no analytical multi-user MIMO channel models are available that directly model the effect of the relative orientation of the channels' eigenspaces (their *alignment*).

Contributions We approach the problem of modeling multi-user MIMO channels via their receiver correlation matrices, which provide two spatial signatures: one for the desired signal, the other for the interference. Our main contribution is a method to *vary the relative orientation of the eigenspaces of multi-user channels in a continuous way*.

We first study a metric that reflect the severity of MIMO interference: interference-impaired mutual information [1]. It can be expressed in terms of the singular values of the receiver correlation matrices and their corresponding eigenspaces. We show that, given the singular values, the metric possesses a specific maximum and minimum, which is achieved in certain

extreme cases of correlation matrix eigenspace alignment.

The main contribution is a way to model the eigenspaces of the multi-user channels. Building on the metric, we present an analytical multi-user MIMO channel model that generates channel realizations according to a user-chosen level of interference severity. This is achieved by continuously rotating the eigenspace of the interference correlation matrix.

Notation The superscript H stands for conjugate (Hermitian) transposition. $\text{E}\{\cdot\}$ denotes the expectation operator, $\text{tr}\{\cdot\}$ the matrix trace, and $\|\cdot\|_{\text{F}}$ the Frobenius norm. \mathbf{I} is the identity matrix of appropriate size. For a matrix $\mathbf{X} = [\mathbf{x}_1, \dots, \mathbf{x}_N]$, we define the notation $\tilde{\mathbf{X}} = [\mathbf{x}_N, \dots, \mathbf{x}_1]$, which reverses the order of the columns. We use the word “metric” in the general sense of a scalar function that quantifies an aspect of interest, not in the mathematically rigorous sense of metric spaces.

Organization Section II introduces the multi-user MIMO metric of interest, which is used in Section III as a basis for the multi-user MIMO channel model. Section IV presents the parameterization of the model from measurements. Finally, we draw conclusions in Section V.

II. METRIC FOR MU-MIMO SYSTEM PERFORMANCE

First, we quantify the impact of different subspace alignment to be able to model it accordingly.

A. System model

We model an interference-impaired MIMO link as depicted in Figure 1 by

$$\mathbf{y} = \mathbf{H}_0 \mathbf{x}_0 + \sum_{i=1}^N \mathbf{H}_i \mathbf{x}_i + \mathbf{n}, \quad (1)$$

where \mathbf{H}_0 denotes the channel matrix carrying the intended signal, \mathbf{H}_i denotes the N interfering channels, and $\mathbf{n} \sim \mathcal{CN}(0, \sigma^2 \mathbf{I})$ is complex white Gaussian noise. We assume that the transmitted symbols are uncorrelated and have unit variance, i.e., $\text{E}\{\mathbf{x}_i \mathbf{x}_i^{\text{H}}\} = \mathbf{I}$, for $i \in \{0, \dots, N\}$. The channel matrices are of dimensions $D \times T_i$, i.e. the number of transmit antennas can vary between the different links.

We define the $D \times D$ channel correlation matrices at the receiver as

$$\begin{aligned} \mathbf{R}_0 &= \text{E}\{\mathbf{H}_0 \mathbf{H}_0^{\text{H}}\}, \\ \mathbf{R}_1 &= \text{E}\left\{\sum_{i=1}^N \mathbf{H}_i \mathbf{H}_i^{\text{H}}\right\}. \end{aligned}$$

Furthermore, we write the eigenvalue decompositions of \mathbf{R}_0 and \mathbf{R}_1 as

$$\begin{aligned} \mathbf{R}_0 &= \mathbf{U} \mathbf{\Lambda} \mathbf{U}^{\text{H}}, \\ \mathbf{R}_1 &= \mathbf{V} \mathbf{\Gamma} \mathbf{V}^{\text{H}}, \end{aligned}$$

where \mathbf{U} and \mathbf{V} are unitary matrices, and $\mathbf{\Lambda} = \text{diag}(\lambda_1, \dots, \lambda_D)$, $\mathbf{\Gamma} = \text{diag}(\gamma_1, \dots, \gamma_D)$ with sorted eigenvalues $\lambda_1 \geq \lambda_2 \geq \dots \geq 0$ and $\gamma_1 \geq \gamma_2 \geq \dots \geq 0$.

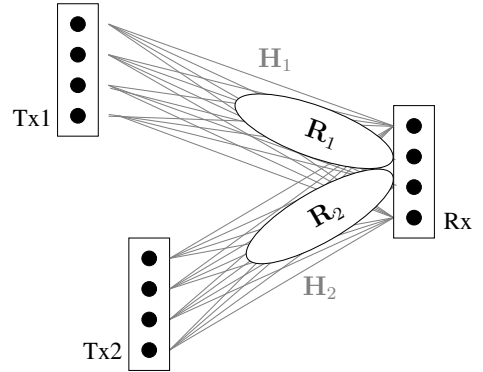


Fig. 1. Multi-user channel from two MIMO Tx to a single MIMO Rx. The individual MIMO channels are denoted by $\mathbf{H}_1, \mathbf{H}_2$. The receive correlation matrices are then given by $\{\mathbf{R}_i = \text{E}\{\mathbf{H}_i \mathbf{H}_i^{\text{H}}\}\}$ for $i \in \{1, 2\}$. Note that whenever the two transmitters are not co-located, these receive correlation matrices will differ significantly.

B. MIMO mutual information with interference

Assuming Gaussian signaling at all transmitters, perfect channel state information at the receivers, and single-user detection (treating the interference as noise), the relevant expected mutual information between input \mathbf{x}_0 and the output \mathbf{y} of the interference-impaired channel in (1) is given by [1]

$$I = \text{E}\left\{\log_2 \det \left(\mathbf{I} + \mathbf{H}_0 \mathbf{H}_0^{\text{H}} (\sum_i \mathbf{H}_i \mathbf{H}_i^{\text{H}} + \sigma^2 \mathbf{I})^{-1} \right)\right\}. \quad (2)$$

Motivated by this equation, we use the correlation matrices \mathbf{R}_0 and \mathbf{R}_1 instead of the channel matrices¹ and define the mutual information metric

$$\begin{aligned} J(\mathbf{R}_0, \mathbf{R}_1, \sigma^2) &= \log_2 \det \left(\mathbf{I} + \mathbf{R}_0 (\mathbf{R}_1 + \sigma^2 \mathbf{I})^{-1} \right) \\ &= \log_2 \det \left(\mathbf{I} + \mathbf{\Lambda} \mathbf{U}^{\text{H}} \mathbf{V} (\sigma^2 \mathbf{I} + \mathbf{\Gamma})^{-1} \mathbf{V}^{\text{H}} \mathbf{U} \right) \end{aligned}$$

where $\mathbf{U}^{\text{H}} \mathbf{V}$ is a unitary coordinate transformation.

It turns out that for fixed eigenvalues, the value of $J(\mathbf{R}_0, \mathbf{R}_1, \sigma^2)$ depends on the degree of alignment between the subspaces characterized by \mathbf{U} and \mathbf{V} . For fixed $\mathbf{R}_0 = \mathbf{U} \mathbf{\Lambda} \mathbf{U}^{\text{H}}$ and $\mathbf{\Gamma}$,

$$\underbrace{J(\mathbf{R}_0, \mathbf{U} \mathbf{\Gamma} \mathbf{U}^{\text{H}})}_{J_{\min}(\mathbf{R}_0, \mathbf{\Gamma})} \leq J(\mathbf{R}_0, \mathbf{V} \mathbf{\Gamma} \mathbf{V}^{\text{H}}) \leq \underbrace{J(\mathbf{R}_0, \tilde{\mathbf{U}} \mathbf{\Gamma} \tilde{\mathbf{U}}^{\text{H}})}_{J_{\max}(\mathbf{R}_0, \mathbf{\Gamma})},$$

for all unitary matrices \mathbf{V} . (For brevity, we omit the parameter σ^2 .) In other words, the two extreme cases are realized by $\mathbf{V} = \mathbf{U}$ and $\mathbf{V} = \tilde{\mathbf{U}}$.

Intuitively, the worst case interference occurs when the eigenspaces of signal and interference are identical and thus, the strongest interference mode affects the strongest signal mode. Conversely, the best case (corresponding to the largest

¹Unfortunately, the usual way to bound the mutual information by pulling the expectation into the $\log_2 \det$ expression is unavailable when interference comes into play. Still, the following equation is a meaningful representation of interference, as will become clear in Section III-C.

mutual information metric) occurs when the strongest eigenmode of the interference aligns with the weakest eigenmode of the signal and vice versa.

To emphasize the role of the subspace alignment, we define the scaled metric

$$\tilde{J}(\mathbf{R}_0, \mathbf{R}_1) = \frac{J(\mathbf{R}_0, \mathbf{R}_1) - J_{\min}(\mathbf{R}_0, \mathbf{\Gamma})}{J_{\max}(\mathbf{R}_0, \mathbf{\Gamma}) - J_{\min}(\mathbf{R}_0, \mathbf{\Gamma})}, \quad (3)$$

which satisfies

$$0 \leq \tilde{J}(\mathbf{R}_0, \mathbf{R}_1) \leq 1. \quad (4)$$

In Section III-C, we demonstrate the relevance of the scaled metric \tilde{J} by example. The metric \tilde{J} is very practical since it directly describes the ultimate performance limits given a certain interference. Note that this approach can be extended to include transmit precoding by including the corresponding precoding matrix into the mutual information equation as demonstrated in [1].

C. Other metrics

The metric \tilde{J} is a specific way to model channel interaction in interference-impaired MIMO communication. Apart from this particular choice, the model proposed in the next section works with any alternative metric that fulfills the following requirements:

- The metric depends on $\mathbf{R}_0 = \mathbf{U}\mathbf{\Lambda}\mathbf{U}^H$ and $\mathbf{R}_1 = \mathbf{V}\mathbf{\Gamma}\mathbf{V}^H$.
- For fixed $\mathbf{R}_0 = \mathbf{U}\mathbf{\Lambda}\mathbf{U}^H$ and $\mathbf{\Gamma}$, it reaches its extreme values for $\mathbf{V} = \mathbf{U}$ and $\mathbf{V} = \tilde{\mathbf{U}}$.
- The metric is continuous in \mathbf{V} .

III. MODELING THE MULTI-USER CHANNEL SUBSPACES

A. Modeling principle

Upper and lower bounds on system performance under several metrics, such as the ones defined in the previous section, are determined by the eigenvalue structure of the receiver correlation matrices. The actual performance, however, is strongly affected by the relative alignment of their eigenspaces as captured by the coordinate transform $\mathbf{U}^H\mathbf{V}$. In order to test MU-MIMO algorithms for their performance, they need to be evaluated under varying channels conditions that cover the entire spectrum of possible signal subspace alignments.

The procedure presented in this section generates receiver correlation matrices for this purpose. Recall that the received spatial signatures are $\mathbf{R}_0 = \mathbf{U}\mathbf{\Lambda}\mathbf{U}^H$ and $\mathbf{R}_1 = \mathbf{V}\mathbf{\Gamma}\mathbf{V}^H$. We assume that the spatial signature \mathbf{R}_0 of the desired signal, the eigenvalue profile $\mathbf{\Gamma}$ of the interference, and the noise power σ^2 , are pre-specified. They may be obtained from measurements or from a qualified link model.

In addition, a target point for the alignment of the subspaces needs to be specified. The alignment is quantified by the metric \tilde{J} within the bounds of (4). Our model generates a suitable \mathbf{V} such that the metric meets the target, i.e., the pre-specified \mathbf{R}_0 and the generated \mathbf{R}_1 are related as desired.

In the following, we describe the procedure in detail for the mutual information metric \tilde{J} , but it applies likewise for

any metric that satisfies the requirements of Section II-C. The procedure can in principle also be used to generate channel matrices instead of correlation matrices.

B. Generation of \mathbf{V}

Assume we are given $\mathbf{R}_0 = \mathbf{U}\mathbf{\Lambda}\mathbf{U}^H$, $\mathbf{\Gamma}$, and $\tilde{J}_{\text{target}}$. Our algorithm finds a \mathbf{V} that satisfies $\tilde{J}(\mathbf{R}_0, \mathbf{V}\mathbf{\Gamma}\mathbf{V}^H) = \tilde{J}_{\text{target}}$.

A solution exists only if $0 \leq \tilde{J}_{\text{target}} \leq 1$. Recall that $\tilde{J} = 0$ is achieved by $\mathbf{V} = \mathbf{U}$, while $\tilde{J} = 1$ is attained by $\mathbf{V} = \tilde{\mathbf{U}}$. Therefore, a \mathbf{V} that meets $\tilde{J}_{\text{target}}$ must exist along a smooth unitary curve from \mathbf{U} to $\tilde{\mathbf{U}}$. Such a curve can be defined as

$$\mathbf{V}(s) = \left(\tilde{\mathbf{U}}\mathbf{U}^H \right)^s \mathbf{U},$$

using the eigenvalue decomposition $(\tilde{\mathbf{U}}\mathbf{U}^H)^s = \mathbf{W}e^{js\mathbf{\Phi}}\mathbf{W}^H$ in which $\mathbf{\Phi} = \text{diag}(\phi_1, \dots, \phi_n)$ is a diagonal matrix of phase angles in $(-\pi, \pi]$. This leads to $\tilde{J}(s)$ being a continuous function. Since $\tilde{J}(0) = 0$, and $\tilde{J}(1) = 1$, the existence of an $s^* \in [0, 1]$ with $\tilde{J}(s^*) = \tilde{J}_{\text{target}}$ is guaranteed. This s^* can be calculated to arbitrary precision by the bisection method [7]. The desired subspace matrix is then $\mathbf{V}(s^*)$.

C. Numerical example

To demonstrate the effect of subspace alignment on system performance, and to illustrate the path-based methods of Section III-B, we consider the following example. Assume the simple receiver correlation structure [8]

$$\mathbf{R}_0 = \begin{bmatrix} \mu^0 & \mu^1 & \dots & \mu^{D-1} \\ \mu^1 & \mu^0 & \ddots & \vdots \\ \vdots & \ddots & \ddots & \vdots \\ \mu^{D-1} & \dots & \mu^1 & \mu^0 \end{bmatrix} = \mathbf{U}\mathbf{\Lambda}\mathbf{U}^H,$$

where the inter-antenna correlation μ ranges between 0.1 (uncorrelated channels) and 0.9 (highly correlated channels).

To model the interference, we use $\mathbf{\Gamma} = \mathbf{\Lambda}$ for simplicity. To demonstrate the impact of the eigenstructure of interference on the capacity of MIMO systems we generate $\mathbf{V}(s)$ as described in Section III-B, varying s from 0 to 1, thus covering the best and worst case. For comparison, we choose $\mu \in \{0.1, 0.5, 0.9\}$ to show the performance differences of changing subspace alignments. The MIMO channels are generated using the (single-sided) Kronecker model [9], i.e., $\mathbf{H}_0 = \mathbf{R}_0^{1/2}\mathbf{G}_0$, and $\mathbf{H}_i = \mathbf{R}_1^{1/2}\mathbf{G}_i = \mathbf{V}\mathbf{\Gamma}^{1/2}\mathbf{G}_i$, where \mathbf{G}_0 and \mathbf{G}_i are complex Gaussian i.i.d. matrices with zero mean and unit variance. Furthermore, we assume the signal and interfering channels to have the same power on average, having both a signal-to-noise ratio of 20 dB.

Figure 2 plots the expected mutual information under interference (c.f. (2)) derived from Monte-Carlo simulations using the generated channels. Note how strongly the expected mutual information changes solely due to the rotations of the interference eigenspace, when channels are correlated. For low correlations ($\mu = 0.1$) changes are almost invisible, however, for higher correlation values of $\mu = 0.9$, changes of more than 65 % are possible.

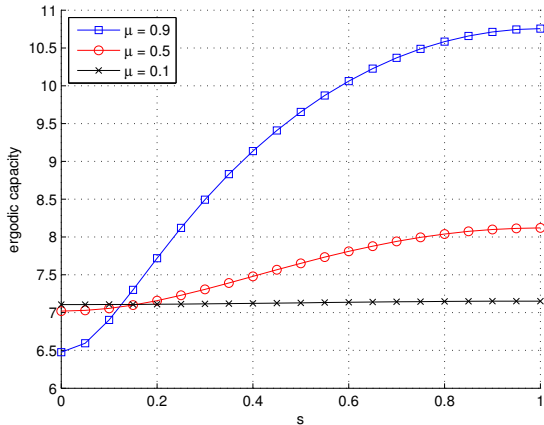


Fig. 2. Ergodic capacity of multi-user interference channels with different alignments of signal and interference subspace. For $s = 0$, signal and interference subspace are completely overlapping, while for $s = 1$, the strongest interference eigenvector couples into the weakest signal eigenvector.

Finally, we demonstrate the relevance of the mutual information metric (3) and its connection to the expected mutual information. For that, we define the minimum and maximum expected mutual information, I_{\min} and I_{\max} as follows: I_{\min} is the expected mutual information when modeling \mathbf{H}_i using $\mathbf{R}_i = \mathbf{U}\mathbf{F}\mathbf{U}^H$, and I_{\max} is the expected mutual information when modeling \mathbf{H}_i using $\mathbf{R}_i = \tilde{\mathbf{U}}\tilde{\mathbf{F}}\tilde{\mathbf{U}}^H$. Using this definition, we define the *scaled* expected mutual information as in (3), but replacing J by I .

Both the scaled expected mutual information and the mutual information metric (3) are plotted in Figure 3 for different singular value profiles. The results show that both lines almost coincide. The barely visible variations are due to the averaging of the expected mutual information. Hence, our metric perfectly captures the changes of ergodic capacity of the channel realizations.

This example demonstrated that subspace alignment needs to be considered for multi-user modeling. The question remains, how strongly realistic channels are separated, and how to model them, which is discussed in the next section.

IV. PARAMETERIZATION FROM MEASUREMENTS

In this section, we demonstrate by an example how the multi-user MIMO model can be parameterized from radio channel measurements.

A. Environment

The example setup is based on indoor-to-outdoor MIMO channel measurements in a 4×2 configuration, where 2-antenna transmitters were moved indoors along well-defined routes [10], as illustrated in Figure 4. The receiver had 4 antennas and was located outdoors approximately 45 m away from the office building at a height of 10 m. The latter is a cubicle-style office environment in Santa Clara, California. The Stanford RUSK channel sounder was operated at a center frequency of 2.45 GHz with a bandwidth of 70 MHz.

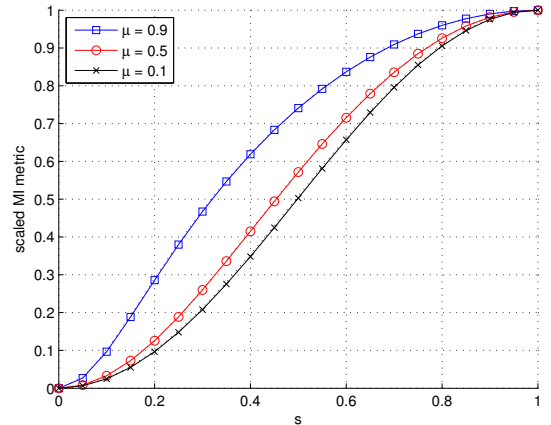


Fig. 3. Mutual information metric \tilde{J} (solid lines) and scaled expected mutual information (dotted lines). The scaled expected mutual information perfectly follows the metric.

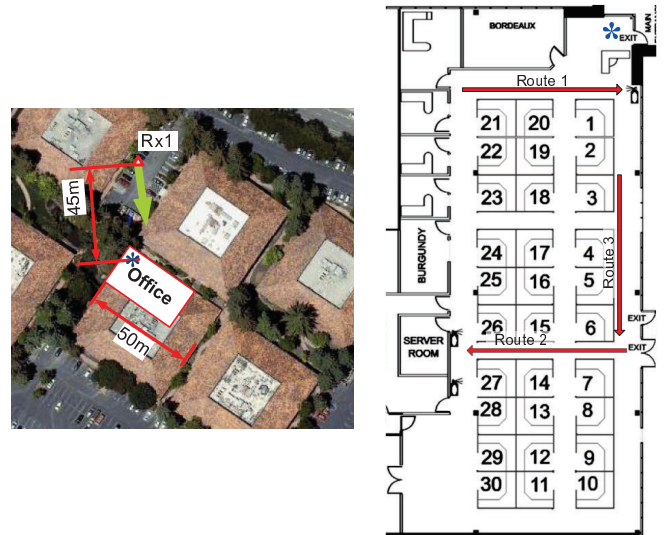


Fig. 4. Indoor-to-outdoor environment and indoor floor plan. The asterisk denotes the matching corner.

B. Parameter estimation

Receive correlation matrices were estimated from the radio channel data of each individual link using a sliding window over short-term stationary periods. Exact details are provided in [10].

As a parameter for the subspace alignment model, we use the *distribution of \tilde{J}* over all distinct links pairs. It is well approximated by a Beta distribution,

$$p_{\beta}(\tilde{J}) = \frac{\Gamma(a+b)}{\Gamma(a)\Gamma(b)} \tilde{J}^{a-1} (1-\tilde{J})^{b-1}$$

where $\Gamma(\cdot)$ is the Gamma function. The Beta distribution is particularly adequate to describe the metric statistics, as it is bounded between 0 and 1, analogous to \tilde{J} . The distribution of the mutual information metric for both investigated pairs

of links is depicted in Figure 5, together with their respective Beta distribution fit:

- for multi-user links with \mathbf{R}_0 evaluated from route 1, and \mathbf{R}_1 evaluated from route 3, $a = 6.31$, $b = 7.90$,
- for multi-user links with \mathbf{R}_0 evaluated from route 2, and \mathbf{R}_1 evaluated from route 3, $a = 6.47$, $b = 38.5$.

Interestingly, the distance between links 2 and 3 (in terms of \tilde{J}) is significantly smaller than the distance between links 1 and 3. Intuitively, this means that both transmitters (on links 2 and 3) communicate towards the outdoor receiver via the same propagation paths, probably through the right-side wall. By contrast, the signals transmitted on routes 1 and 3 reach the outdoor receiver through different propagation paths. Given the environment layout, one may safely assume that the main propagation path on route 1 is through the upper right corner (indicated by the asterisk) directly to the receiver, whereas on route 3, propagation mostly takes place through the right-side wall and then diffraction on a neighboring building towards the receiver. Hence, routes 1 and 3 are well separated, since the corresponding propagation paths do not significantly intersect from the outdoor receiver viewpoint.

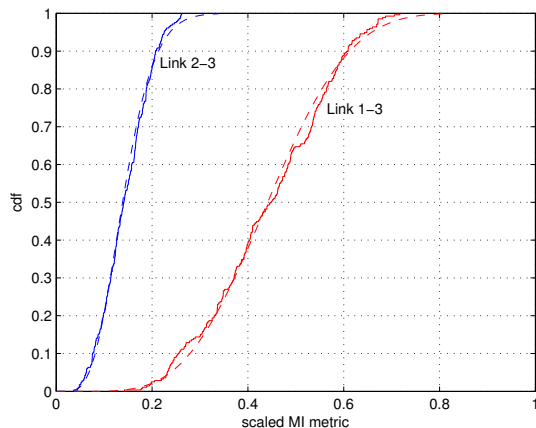


Fig. 5. Empirical (solid line) and fitted Beta (dashed line) distributions of \tilde{J}

As a consequence, the eigenvalue distributions for all three investigated links might differ substantially. Hence, they are evaluated separately. We found that all eigenvalue distributions could be well approximated by a lognormal distribution. The mean and standard deviation of the best-fit Gaussian distributions are summarized in Table I.

It can be observed that the eigenvalue distributions on links 2 and 3 are actually quite similar, while being largely different on route 1. This confirms the previous discussion on the differentiated propagation paths, i.e., that the main propagation path for links 2 and 3 is via the right-side wall, in contrast to link 1.

V. CONCLUSIONS

We presented an analytical multi-user MIMO channel model that is able to model interference in the spatial domain.

TABLE I. Eigenvalue distributions in indoor-to-outdoor scenarios

Link index	Sorted eigenvalue index	Mean (dB)	Std (dB)
1	1	4.09	0.68
	2	-0.78	1.53
	3	-4.89	1.84
	4	-8.12	1.60
2	1	3.63	0.40
	2	0.03	0.63
	3	-3.75	0.95
	4	-6.37	0.92
3	1	3.18	0.53
	2	0.07	0.71
	3	-2.42	0.99
	4	-5.61	1.16

The proposed model characterizes the amount of eigenspace alignment on a continuous scale between fully aligned and maximally non-aligned.

The parameterization of the model is exemplified using channel measurements in an indoor-to-outdoor cubicle-style office environment. We demonstrated that in real environments, the effect of interference indeed depends heavily on its alignment with the desired signal space.

It turns out that system performance metrics under interference strongly depends on the alignment of the eigenspaces of the channel matrices of the intended signal and of the interfering channel. For strongly correlated channels, the difference in data rate can reach up to 65 % in a 4×4 MIMO system.

REFERENCES

- [1] R. Blum, "MIMO capacity with interference," *IEEE Journal on Selected Areas in Communications*, vol. 21, no. 5, pp. 793–801, 2003.
- [2] Y. Liu, T. Wong, and W. Hager, "Training signal design for estimation of correlated MIMO channels with colored interference," *Signal Processing, IEEE Transactions on*, vol. 55, no. 4, pp. 1486–1497, 2007.
- [3] X. Chen, Y. Gong, and Y. Gong, "Suppression of directional interference for STBC MIMO system based on beam-forming," in *Communications, Circuits and Systems Proceedings, 2006 International Conference on*, vol. 2, 2006, pp. 983–987.
- [4] M. Rahman, E. de Carvalho, and R. Prasad, "Mitigation of MIMO co-channel interference using robust interference cancellation receiver," in *Vehicular Technology Conference (VTC Fall 2007)*, Baltimore, MD, USA, October 2007.
- [5] T. Fügen, J. Maurer, C. Kuhnert, and W. Wiesbeck, "A modelling approach for multiuser MIMO systems including spatially-colored interference [cellular example]," in *IEEE Global Telecommunications Conference, 2004. GLOBECOM '04.*, vol. 2, 2004, pp. 938–942 Vol.2.
- [6] J. Poutanen, F. Tufvesson, K. Haneda, V.-M. Kolmonen, and P. Vainikainen, "Multi-link MIMO channel modeling using geometry-based approach," *IEEE Trans. Ant. Prop.*, 2011, in press.
- [7] R. W. Hamming, *Numerical Methods for Scientists and Engineers*. Dover Publications, 1987.
- [8] C. Martin and B. Ottersten, "Asymptotic eigenvalue distributions and capacity for MIMO channels under correlated fading," *IEEE Trans. Wireless Commun.*, vol. 3, no. 4, pp. 1350–1359, July 2004.
- [9] C. Oestges and B. Clerckx, *MIMO Wireless Communications*. Elsevier Academic Press, 2007.
- [10] N. Czink, B. Bandemer, G. Vazquez-Vilar, L. Jalloul, C. Oestges, and A. Paulraj, "Spatial separation of multi-user mimo channels," in *IEEE PIMRC 2009*, Tokyo, Japan, September 2009.